The significance of sub-grid scale orography and problems in their representation in GCM's

François LOTT*

ECMWF, Shinfield Park, Reading, Berkshire RG2 9AX, England.

September 1994

Abstract

The problem of representing Subgrid Scale Orography (SSO) in General Circulation Models (GCM) and Numerical Weather Prediction Models (NWPM) is reviewed. In the first part, a very accurate dataset (185mx185m) of the Alps is used to evaluate the impact of the different scales of the SSO on the general circulation of the atmosphere. From a linear point of view, the mountain features which horizontal scale varies between few Km and 100Km excite gravity waves which can transfer angular momentum between the orography and the atmosphere. It is also shown, evaluating their impact on the general circulation of the atmosphere that these waves have to be parameterized in GCM and in accurate global NWPM. Allthough instructive, this linear approach is not really justified for mountain peaks as high as those existing in the Alpine region. At the scale of the gravity waves, it means that upstream blocking, low level wave breaking with non-linear wave reflection at the overturning region and flow splitting around

*Present affiliation: Laboratoire de Météorologie Dynamique du CNRS, Ecole Normale Supérieure, 24 rue Lhomond, 75231 Paris Cedex 05, France

the obstacle occur. These different effects lead to drags significantly larger than the gravity wave drag. Present efforts in representing the SSSO in GCM try to consider this nonlinear enhancement of the drag. For smaller scales peaks (between few 100m and few Km), the nonlinearity means that bluff body separation near the summit occurs which lead to drags as large as the gravity wave drag. This effect is partly taken into account in the boundary layer scheme, when the roughness length is increased over montaneous area. It is noteworthy that those two different nonlinear effects, mainly concern the the low level flow and the envelope orography can be viewed as a way to parameterize them.

In the second part, the beneficial impact of two aspects of the SSO parameterization (i.e., the envelope orography and the gravity wave drag scheme) is reviewed following the literature on the subject. Nevertheless, to actualize the results, only recent seasonal T63L19 integration and T106L31 10-days forecast are discussed. At the sub-synoptic scale, important default of those different parameterization can be found when comparing to field measurements (PYREX), showing that significant progresses have to be made in the tuning of the various SSO representation.

1 INTRODUCTION

In the present numerical models of the atmospheric general circulation, there are three different ways of representing the SSO One is the parameterisation of the gravity waves (Boer et al., 1984; Palmer et al., 1986) which has led to improve the simulation of the tropospheric winter's jet in the north-hemisphere at high altitudes. Theoretically, the existence of these waves comes immediatly out of the linearized equation of motion of a stratified fluid above an irregular bottom (Queney, 1947) . Their existence were confirmed by measurements (Lilly et al., 1982; Bougeault et al., 1993) . The second representation of the SSO is the parameterization of the boundary layer structure above hilly terrain (Tibaldi and

Geleyn, 1981; Mason, 1985) by increasing the roughness length over mountaneous areas. Theoretically, it represents the pressure drag exerted by a hill on a turbulent flow over it (Taylor, 1977) . In a more nonlinear context, Wood and Mason (1993) further showed that the enhancement of the turbulent friction resulting from flow detachement alee of the summits of sharp mountains, can lead to drags, which are as large as the gravity wave drags, and which can also be parameterized using large roughness length. The realism of this parameterisation was further confirmed by measurements (Grant and Mason, 1990) . Contrary to the gravity wave drag schemes, this kind of parameterization was not introduced to reduce some well defined systematic errors of models, but resulted from an intuitive need to increase surface drag in models above mountaneous area. The third representation of the SSO is the envelope orography. It consists in enhancing the model mean orography by a factor which is geographically dependant on the standard deviation of the SSO. The main objective of this parameterization is to reduce explicitely systematic errors in the ECMWF forecasting systems. At the opposite of the preceding parameterization, it is the theoretical and observational justifications, which stand that with mean orography models underestimate large scale blocking upwind of large massifs, which are more intuitive (Wallace et al., 1983) .

The development of these different parameterizations was made relatively independantly one from the other. Naturally, this is not really justified and the distinction between them is rather arbitrary, allthough funded over a simple horizontal scale argument: the increase roughness length parameterizes small scale orography, the gravity wave drag parameterizes the mesoscale orography and the enveloppe orography parameterizes the lack in the representation of the synoptic scale orography. In reality, and essentially because the atmosphere is dominated by nonlinear effects which make invalid this scale separation, it is clear that the mesoscale dynamics over mountain certainly depends on the low level boundary layer structure and that the envelope orography which induces some

drag may partly be viewed as a gravity wave drag parameterization.

The purpose of the present study is to give a comprehensive review of these three different parameterizations used in GCM and NWPM. In the section 2 of this paper, a very accurate dataset of the Alps is used to give a general justification of the three parameterizations described before. In the Section 2.1, a very simple (linear) dynamical analysis of this dataset naturally lead at the first order to the concept of gravity waves. Calculation of the related mountain waves drag in a typical configuration show that the Alps alone can have an significant impact on the general circulation of the atmosphere. As a consequence, the parameterization of mountains in GCM can not be neglected. Nevertheless, the same dataset shows that this linear approach is not appropriate. The Section 2.2 discuss some nonlinear effects using two limit conceptual models. The first one is that of stable or slow flow, which in the literature was studied in the context of nonlinear mountain waves. The second one is that of neutral or fast flow, in the literature it was studied in the context of the interaction between the boundary layer and the orography. The concept of envelope orography appears as an artefact to simulate at large scale the impact of these nonlinear processes, which essentially slow down and mix the flow at low level. In the Section 3, the impacts of two of these parameterization (the envelope orography and the gravity wave drag) are reviewed following the literature on the subject, but diagnosing recent seasonal integration and 10 days forecasts done with the ECMWF model. In Section 3.4 some comparison between these parameterizations and field data (PYREX, citeboueta93) are discussed. At the scale of the Pyrennes, and for the ECMWF model at truncature T213, it becomes quite clear that the distinction between the gravity wave drag parameterization and the envelope orography is not really justified. In the conclusion, we further insist on the scale interdependance of these different parametrizations of the SSO, emphasizing on the relationships between the mesoscale orography parametrization and the parameterization of the atmospheric turbulence.

2 GENERAL CONSIDERATIONS

One of the fundamental problem in representing the impact of orography in GCM and in NWPM is that the earth orography has no preferential horizontal wavenumber. Figure 1 for instance, shows a section of the Alps orography, h(x), along a zonal transect of length L=800Km, located at the latitude $45.9^{o}N$, and according to three different datasets. The first one is a very accurate dataset (185mx185m) close to that presented by Volkert (1990)(hereafter referenced as the IPA [1] dataset). The second one is the USN (10'x10') dataset upon which most of the orographic climate fields are deduced in the ECMWF model. The third is the model orography, explicitely used as a lower boundary condition for the Geopotential height in the T213 ECMWF model with mean orography. It is quite clear that at the range of the Alps the shape of the mountain varies considerably from one dataset to an other one. A typical horizontal extension of the mountain peaks is of the order of 100km for the T213 ECMWF model, 25Km for the USN dataset, and few kilometers for the IPA dataset. In the following, we are going to discuss qualitatively three questions which naturallly come out of this straightforward orographic datasets comparison. Does the model orography represents part of the real orography? Does the scale of the mountains, which are not represented by the model orography, have any impacts on the general circulation of the atmosphere? Is the USN dataset accurate enough to describe the impact of the Subgrid Scale Orography on the General Circulation of the atmosphere?

2.1 A linear point of view

In this subsection, it is assumed that the orography is small enough so that the dynamical answer of the atmosphere to the mountain forcing is linear. In this

[1] Institute fur Physiks der Atmosphare.

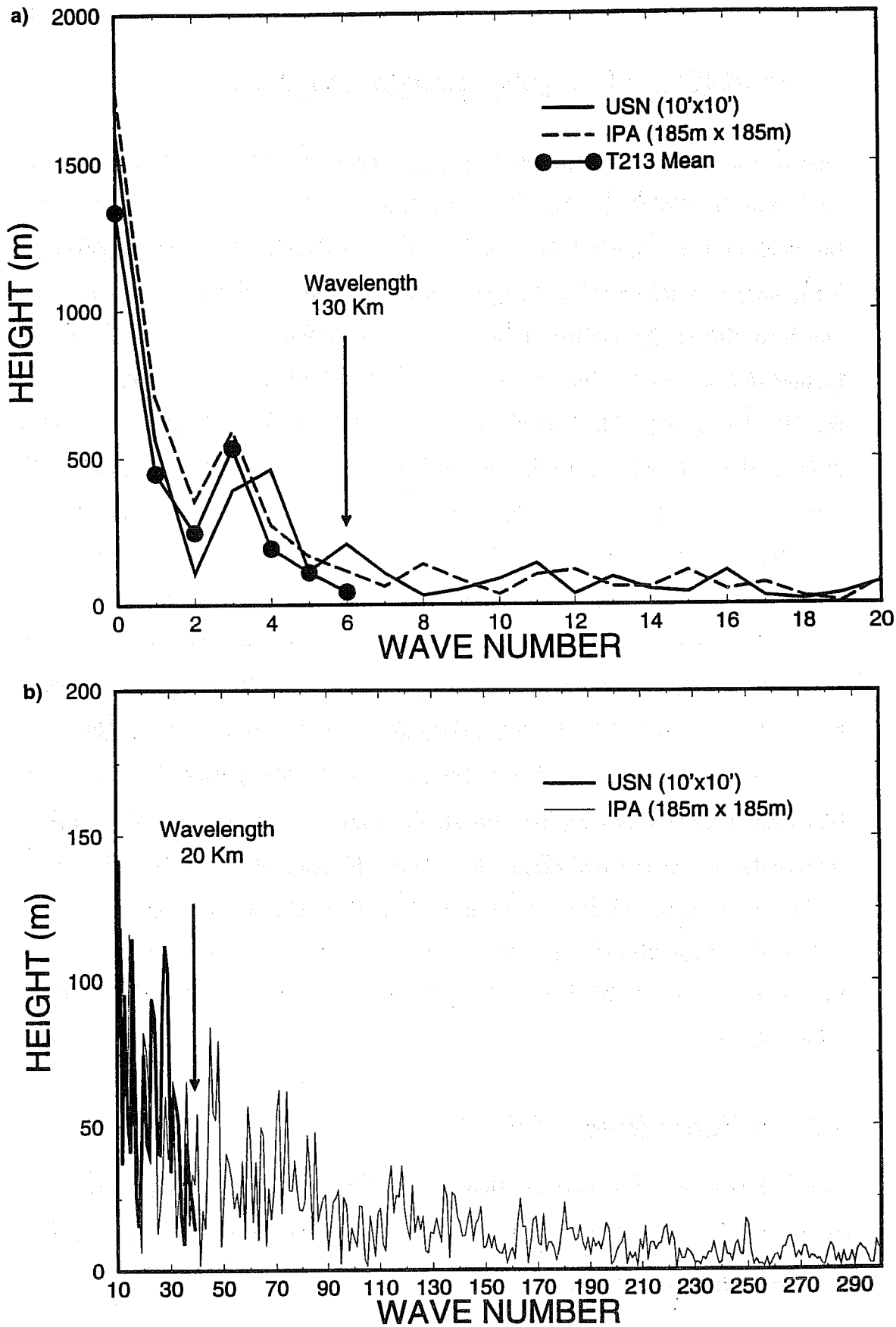

Fig 1 East West section of the Alps at the latitude 45.9° N according to three different datasets: high resolution (185 m x 185 m) dataset provided by the Institute für Physik der Atmosphäre (normal); conventional (10'x10') dataset provided by the US Navy (bold); mean orography in the ECMWF T213 model (bold dotted). (a) Complete alpine section; (b) zoom between longitude 7° E and 9° E.

context, one can develop the solution in harmonics, and look to the behaviour of each wave accordingly. Then, to specify a lower boundary condition, the orography displayed on Figure 1, is expanded in a Fourier Series:

$$h(x) = \sum_{K=0}^{M} H_K \cos(K\frac{2\pi}{L} + \phi_K) \, , \; H_K = \frac{2}{L}\int_0^L h(x)\cos(K\frac{2\pi}{L} + \phi_K)dx \qquad (1)$$

where each harmonic, K, is related to a zonal wavenumber, $k = K\frac{2\pi}{L}$. H_K and ϕ_K, are the wave amplitude and the wave phase associated to this harmonic respectively. L is the length of the Alps section displayed on Figure 1 and M is the highest order harmonic one can extract by fourier transform from each dataset. Typically, $M = \frac{N}{2} - 1$, where N is the number of points available along the transect. For the IPA dataset, this gives more than $M = 2000$ harmonics, while only $M = 29$ harmonics can be extracted from the USN dataset and $M = 6$ harmonics from the T213 model orography. The Figure 2 presents these Fourier coefficients associated to the three orography datasets displayed on Figure 1. The amplitude of the first sixth harmonics of the model mean orography fits quite well with those of both the USN dataset and of the IPA dataset. It means that in the linear context, the model orography correctly forces the part of the wave motion which is related to the mountain scale larger than 100km. From this range to the 29th wavenumber, the mountain spectrum presents a continuum which amplitude and variation are quite well represented by the USN dataset (when compared to the IPA dataset). This range corresponds to waves which horizontal wavelength typically goes from 100km to 25km.

To determine which scales of the Alps can affect the large scale circulation of the atmosphere, it is relevant to analyse which waves, allow a transfert of angular momentum transfert between the Alps and the mean flow. With a lot of simplification, it is assumed that the governing equation for the linear motion forced by the Alps can be written on a f-plane, that the mean wind, U, is zonal,

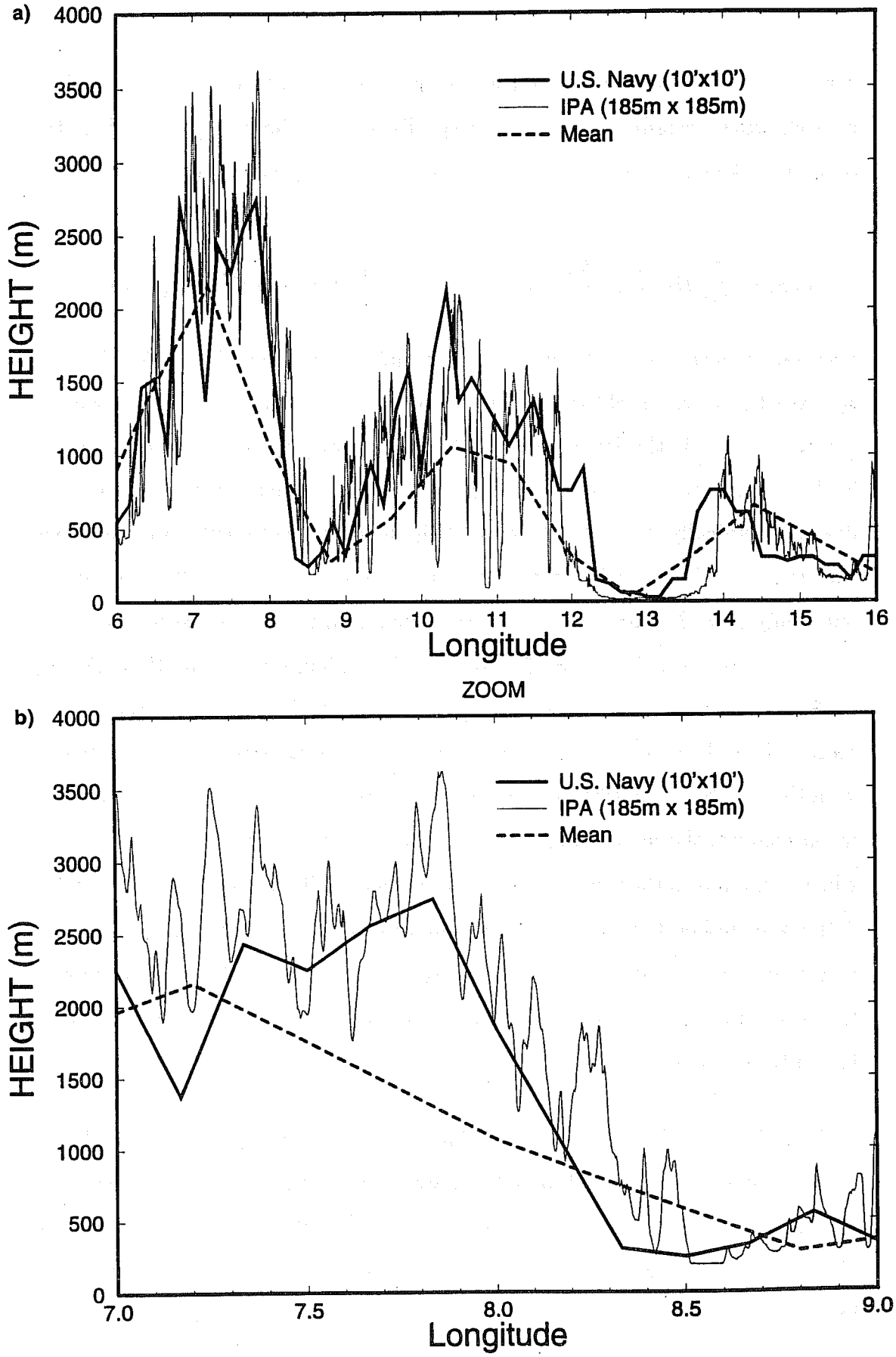

Fig 2 Amplitude of the harmonics of the Alps section display in Fig 1 and according to the same three dataset. (a) Wavenumber 0 to 20; ECMWF T213 model (bold with circle), USN (10'x10') (bold) and accurate 'IPA' dataset (dotted bold). (b) Wavenumber 10 to 290: USN (10'x10') (bold) and accurate 'IPA' dataset (dotted).

independant of height and that the meridional variation of the obstacle on the wave structure can be neglected. In this context, the equation for the amplitude of each modes, $W_K(z)$, of the vertical velocity, $w(x,z)$:

$$\frac{d^2W_K(z)}{dz^2} + k^2\frac{N^2-k^2U^2}{k^2U^2-f^2}W_K(z) = 0 \; with \; W_K(0) = kUH_K \, . \qquad (2)$$

Solving equation (2) and coming back to the physical space, gives:

$$w(x,z) = -\sum_{K=1}^{K_f-1} kUH_K \, e^{-m_K z} \sin(kx+\phi_K) \quad -\sum_{K=K_f}^{K_N} kUH_K \sin(m_K z + kx + \phi_K) \quad -\sum_{K=K_N+1}^{M} kUH_K \, e^{-m_K z} \sin(kx+\phi_K) \qquad (3)$$

where $m_K = k\sqrt{\left|\frac{N^2-k^2U^2}{k^2u^2-f^2}\right|}$ and $(K_f-1)\frac{2\pi}{L} < \frac{f}{U} < K_f\frac{2\pi}{L}$ and $K_N\frac{2\pi}{L} < \frac{N}{U} < (K_N+1)\frac{2\pi}{L}$

Among these different harmonics, only those in the second summation terms of Equation (3) correspond to propagating gravity waves. The other modes are evanescent and decay in the vertical direction. It is now largely established (Gill, 1982; Bretherton, 1969) , that only the propagating modes allow a flux of angular momentum from the earth to the atmosphere. Further details about the redistribution of this momentum flux into the mean flow is given in the following contribution (Mobbs, 1994) . At the ground, this flux is balanced by the pressure drag:

$$D = \frac{1}{L}\int_0^L -p'\frac{dh}{dx} = \frac{1}{2}\sum_{K_f}^{K_N}\rho_0\sqrt{|(N^2-k^2U^2)(k^2U^2-f^2)|}{H_K}^2 \, . \qquad (4)$$

Figure 3 shows the contribution of each wave modes forced by the mountain to the gravity wave drag D when $U = 10ms^{-1}$ and $N = 0.01s^{-1}$. Figure 3 also shows a "white noise" curve which is the function,

$$\sqrt{|(N^2-k^2U^2)(k^2U^2-f^2)|} \, ,$$

modulating the amplitude of each mode of the orography H_K into the wave drag expression (4). It clearly indicates the two cut-off wavenumber $K_f = 2$ and

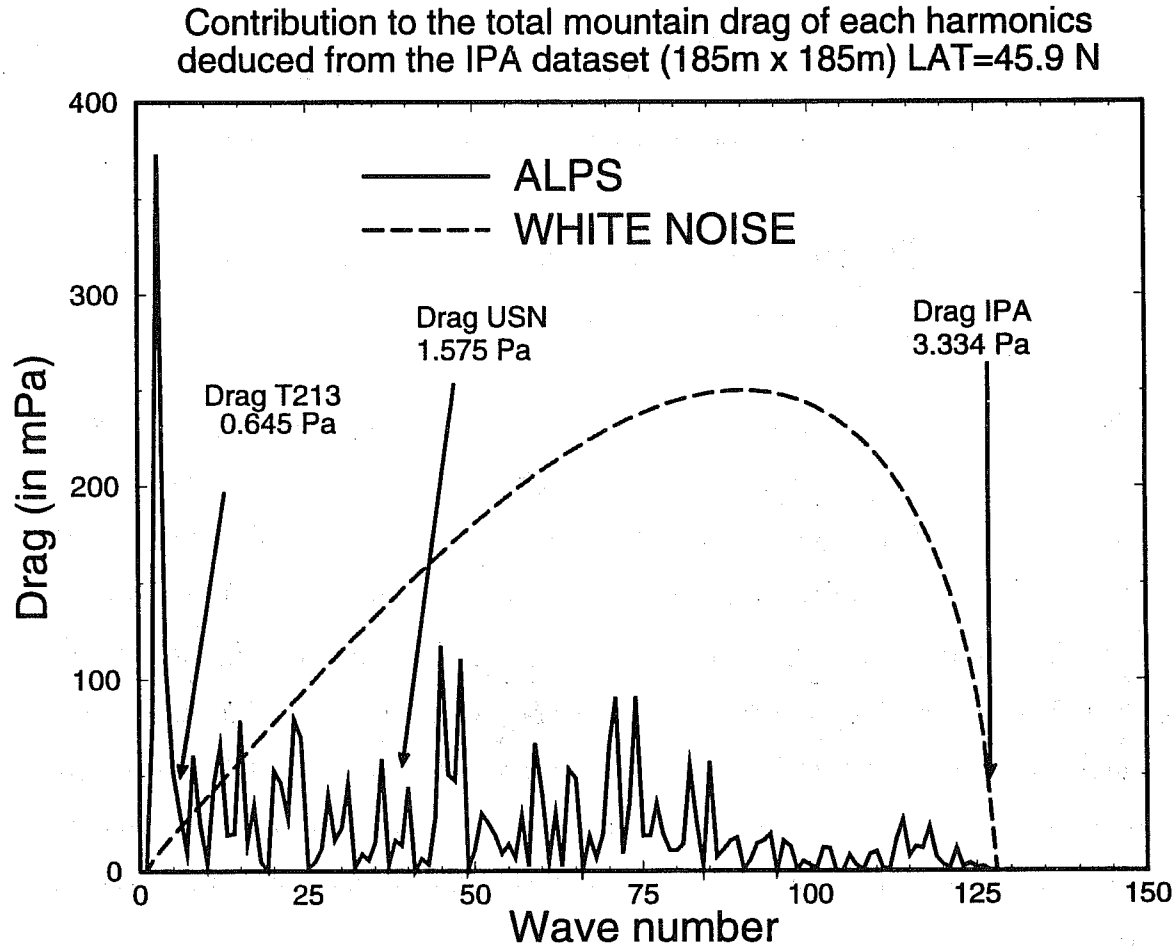

Fig 3 Amplitude of the drag exerted by each mode of the Alps orography (bold). The white noise curve shows the function of the zonal wavenumber, which modulates the mode amplitude in the expression of the drag. The values displayed with arrows show the drag amplitude when the Alps spectrum is truncated at wavenumber 6 to simulate the T213 model mean orography and at wavenumber 30 to simulate the USN orography.

$K_N = 128$, below and beyond which the waves forced by the orography do not contribute to the gravity wave drag. In the flow configuration considered here, the wave drag equals, $D = 3.334Pa$, when the summation (4) is done over all the harmonics provided by the IPA dataset.

The significance of such a drag on the general circulation of the atmosphere can be appreciated evaluating the evaluating the amount of time this drag needs to stop the mean barotropic flow at the latitude considered. This can be done, averaging the zonal momentum equation over the latitude row (Swinbank, 1985) and neglecting the transients. In this case, the tendency for the zonal barotropic flow at the latitude of the Alps reduces to:

$$\frac{dU}{dt} = -\frac{g}{P_s}\frac{L_{Alps}}{L_{Earth}}D \approx 0.24D, \tag{5}$$

when D is expressed in Pascal and the tendency is expressed in m/s/day. In (5), $L_{Alps} \approx 800Km$ and $L_{Earth} \approx 30000Km$, are the lengthes of the Alps and of the meridian at the latitude, 45.9^oN. It means that in the absence of other mechanisms, the Alps would stop the incident flow in 10 days (for a drag of 3Pa). Also very crude since it neglects the essential contribution of the transients, this estimation shows that at short term (less then few days) it seems possible to neglect the drag due to the Alps, at medium range it certainly has a significant impact on the atmospheric circulation.

This estimation shows that in a climatic GCM, for which a massif like the Alps is smoothed out by the coarse model resolution, such a drag can not be neglected. Nevertheless, as it has been discussed before, in an accurate T213 forecasting system, the Alps are roughly represented until the wavenumber 6. The contribution of these modes to the drag (4) gives 0.645Pa. It means that even if the model starts to explicitely solve a part of the gravity wave spectrum, a significant amount of them, still need to be parameterized. Furthermore, when the evaluation of D in (4) is truncated at the wavenumber 29 to simulate the wave

drag one can estimate from the USN dataset, the drag D=1.575Pa. It shows that the USN dataset, upon which most of the parameterization of the SSO is based, is not accurate enough to describe the gravity wave drag.

2.2 Few nonlinear effects

In the linear calculations presented in subsection (2.1), the short modes, with wavelength smaller than 6.28km ($K > 125$), do not contribute to the mountain drag. Nevertheless, this picture is not valid in the non linear context where all the modes may contribute to the interaction between the SSO and the large scale dynamics. To evaluate the validity of the linear approximation it is relevant to come back to the physical space and to analyse the flow structure induced by the individual peaks of the massif. Figure (1b) showing a zoom of the Alps presents this massif as a succession of peaks which typical horizontal length is between 3km and 9Km and which typical height is between 200m an 1500m . To evaluate the validity of the linear approximation, it is relevant to compare a typical vertical scale of the flow disturbance forced by one peak to the peak height, H. For one single isolated obstacle, which horizontal length is, l, equation (3) shows that the forced motion is dominated by a vertical wavenumber (or e-folding decay length),

$$\lambda \approx \frac{U}{N}\sqrt{\left|\frac{1-Ro^{-2}}{1-Fr^2}\right|}. \tag{6}$$

where $Ro = \frac{U}{fl}$ and $Fr = \frac{U}{Nl}$ are a Rossby number and a Froude number respectively. Then, the condition for linearity becomes,

$$\lambda >> H, \ i.e., \ H_{ND}{}^{-1}\sqrt{\left|\frac{1-Ro^{-2}}{1-Fr^2}\right|} >> 1, \ where, \ H_{ND} = \frac{HN}{U}. \tag{7}$$

H_{ND}, being a nondimensional mountain height. For the mountain peaks aforedescribed it is natural to neglect the Rossby number and the Froude number is

close to one. Regarding the value of the Froude number, the flow over a characteristic peak of the Alps is in intermediate configuration between two asymptotic configurations which are described below.

Slow Flow ($Fr << 1$), linear if $H_{ND} << 1$

The first configuration is the stable (or slow flow) configuration for which, $Fr << 1$. In this case, as shown in the subsection 2.1, most of the modes excited by the obstacle are radiating gravity waves and the linearity criteria is simply, $H_{ND} << 1$. Nevertheless, for a typical peak of the Alps, this parameter is of order 1 or even larger. It means that the wave drag mechanisms afordescribed has to be modified to allow for nonlinear effects. Those nonlinear effects can lead to high drag states for which the drag increase can be as large as the linear gravity wave drag (Bacmeister and Pierrehumbert, 1988) . Furthermore the related increase of the drag is related to low level effects, like upstream blocking (Pierrehumbert and B., 1985) , flow splitting around the obstacle (Miranda and James, 1992) and low level breaking gravity waves(Durran, 1987) and nonlinear wave reflection below the overturning layers (Clark and Peltier, 1984) . Those different studies have been essentially developed to explain strong downstream Foehn events and downslope windstorms. It is noteworthy that all these effects tend to affect the flow at levels located below and close to the mountain top.

Fast Flow($Fr >> 1$), Linear if $\frac{H}{L} << 1$

The second configuration is the neutral configuration (or fast flow) for which the advective time scale, $\frac{l}{U}$, is small compared to the buoyancy time scale N^{-1}. Then, the linearity condition (7) reduces to the small slope condition: $\frac{H}{L} << 1$. In the literature the neutral flow configuration was mainly studied in the context of the interaction between the boundary layer and the orography (a neutral flow generally goes with developed turbulence) (Grant and Mason, 1990) . In this

context, the boundary layer drag increase due to the orography is known to be significant when compared to the gravity wave drag amplitude. On Figure 4, the mountain slope calculated from the IPA dataset has been averaged over (10'x10') boxes, so that each of these boxes contain few mountain peaks. For the Alps, this slope parameter has a typical amplitude of 0.4. According to Wood and Mason (1993). it is a large value for which flow separation often occurs at the mountain peaks. Furthermore, for one transect of length L, containing one single ridge, the drag exerted by the flow on this peaks when flow detachment occurs near the summit, follows ce conventional form(Batchelor, 1967) :

$$D_h = \rho_0 D_d \frac{H}{L} \frac{U|U|}{2} \, (Pa) \tag{8}$$

and C_d is a constant of order 1. If we add the contribution of each ridges shown on Figure 1 to obtain the overall aerodynamic drag the Alps experienced when flow detachment occurs at all the peaks gives an aerodynamic drag of

$$D_H = \rho_0 D_d \sum_{i=1}^{P} \frac{H_i}{L} \frac{U|U|}{2} \approx 3Pa \tag{9}$$

In this expression, the parameter P represents the number of peaks, counted along the Alps transect. This hydrodynamic drag has the order of magnitude of the gravity wave drag. On the Figure 4, it is also noteworthy that the evaluation of this slope parameter using the USN dataset (y-axis) leeds to a very large underestimation.

The Concept of Envelope Orography

In the past ten years it has been assumed that the low level processes described in the preceding two chapters, mainly affect the flow at low level, creating sheltered zones where the wind is zero. Once reached a steady states, these sheltered zones remain isolated from the large scale flow if the diffusion processes, are not strong enough to mix the higher layer atmosphere with those sheltered layer.

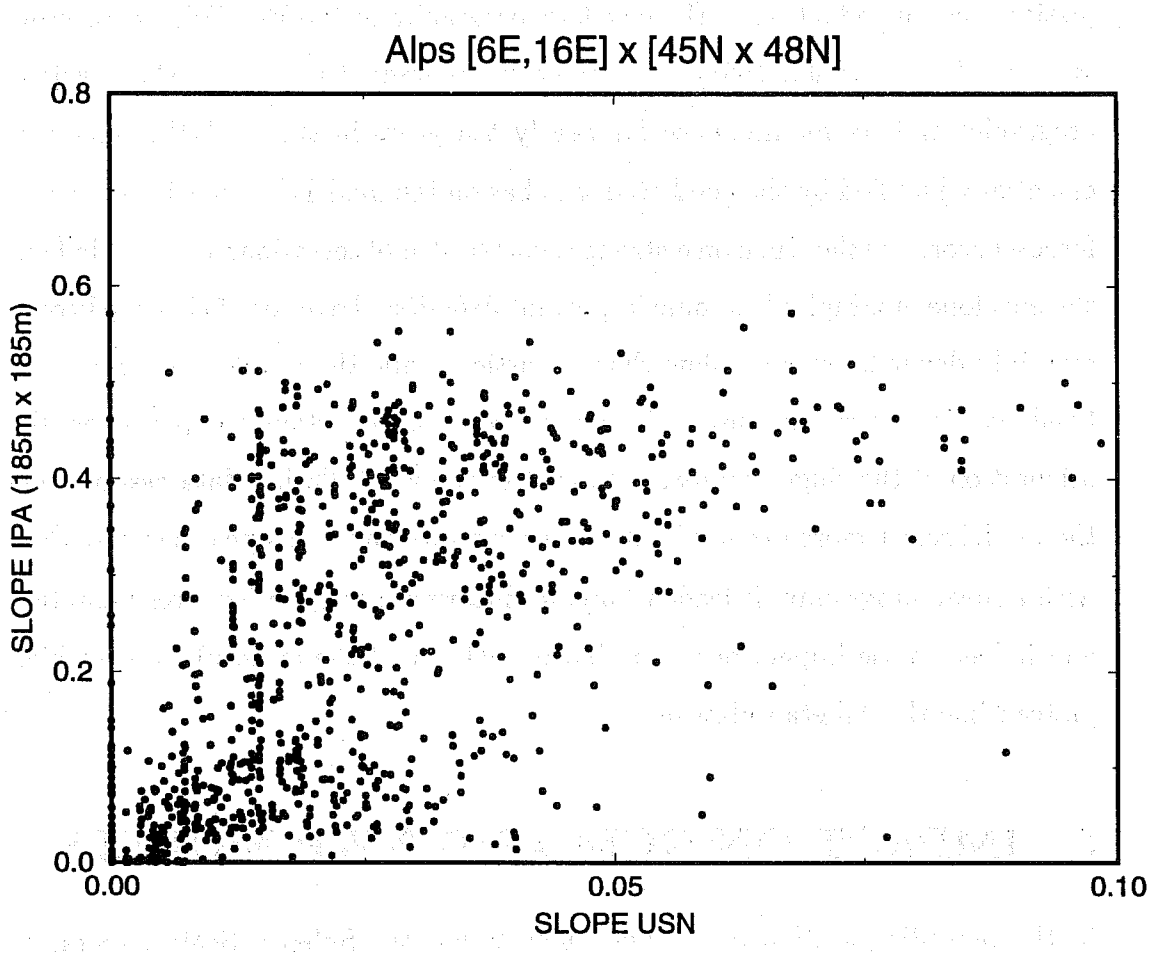

Fig 4 Slope of the mountain averaged over 10'x10' boxes covering all the alpine regions. Y-axis, values deduced from the USN dataset. X-axis: values deduced from the high resolution (IPA) dataset.

If this is the case, the related drag no longer needs to be parameterized once excluded the flow located inside this sheltered zones. These arguments have justified the introduction of the envelope orography in the ECMWF forecasting system (Wallace et al., 1983) . Nevertheless, nowadays the use of the envelope orography and its maintenance for nearly ten years in the ECMWF model is essentially justified by the good results it has on the model systematic errors and forecast scores, rather then on a strong theoretical or observationnal basis. In fact, the envelope orography has some important defaults: the onset of sheltered zones certainly depends on some flow characteristics, while the envelope orography is fixed one for ever; the onset of sheltered zone also certainly depends on the orientation of the ridges compared to that of the wind; during data assimilation the model reject more low level data over land with the envelope orography than with a mean orography; it leads to predict incorrect precipitation over mountain and it has a false impact on the radiation balance of the atmosphere over high plateau like the Tibetan plateau.

3 IMPACT ON GCM AND NWP MODELS

In the preceding section it has been shown that the Subgrid Scale Orography may have a significant impact on the large scale circulation of the atmosphere. If this is the case, numerical models in which these processes are neglected should show some systematic defects in the way they simulate the general circulation of the atmosphere. Since the orography is steady it is conventional, at least in the extratropical regions, to track these defects filtering out high frequency and low frequency patterns. It is also conventional to look at winter configuration (December-January- February) since the orography has a large impact on the dynamics when the westerlies are strong.

3.1 Steady planetary waves and envelope orography

Such a diagnostics is shown on Figure (5a) where the time mean geopotential height of the 500Hpa surface averaged upon five winters (1986-1990) of ECMWF analysis is displayed. The main characteristics features of the northern hemisphere planetary wave pattern, are the ridge over the Rockies, and the pronounced troughs over the eastern sides of the two oceanic basins. One's subjective impression is of predominant zonal wavenumbers 2 and 3. This reinforces the idea that this pattern is mainly due to orography rather than from thermal contrasts betwen land and sea. In fact, Manabe and Terpstra (1974); Held (1983) indicate that the orographic contribution to the stationary wave pattern is mainly in zonal wavenumber 2 and 3. This is also supported by the fact that the pronounced ridge over the Rockies, corresponds to a negative vorticity anomaly similar to that observed by compression of Taylor columns in a simple barotropic model of a flow incident over a circular mountain (see for instance the review of Smith (1979)). The same planetary wave pattern is shown on Figure 5b, but from 5 120 days T63L19 winter integrations. These seasonal integrations start every days of the first 5 days of November 1990, and the model orography is a mean orography (see Wallace et al. (1983) for a description of the design of the orography in the ECMWF model). In this configuration, it is clear that the model does succeed in simulating the major features of the time mean pattern, but it weakens the ridge over the rockies and the trough over the eastern sides of the oceanic basins. It also fails to simulate the split of the flow over western Europe. These defaults make the time-mean flow too zonal. There is also a zonally symmetric error in the simulated flow at $40^0 N$ since the geopotential height gradient is two strong, which means that the westerlies are too strong at this latitude. These weaknesses in the representation of the planetary wave pattern gives the impression that the ECMWF model does not adequatly represent the dynamical influence of the earth's major mountain ranges upon the large scale motion. As shown on

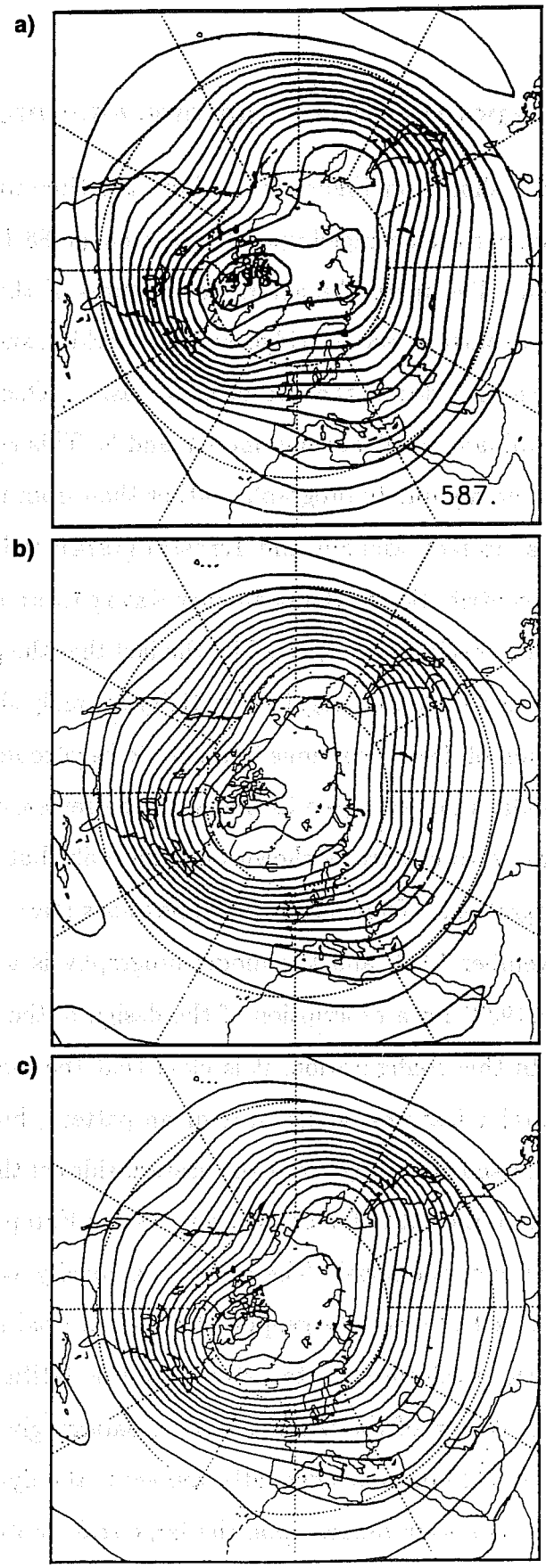

Fig 5 Northern Hemisphere climatic winter (Dec-Jan-Feb) 500 mb geopotential height: winter mean averaged over 5 realisations. (a) Analysis (years 1986 to 1990). (b) 120 day forecast with mean orography (c) 120 day forecast with envelope orography. In (b) and (c), the 5 forecasts correspond to 5 120 day realisations of the ECMWF T63L19 model starting 1, 2, 3, 4 and 5 November 1990. In these forecasts only the last 90 days are analysed to define the model climate.

the Figure 5c, the planetary wave structure with the envelope orography seems substantially improved when compared to that obtained from mean orography simulations. Particularly, the ridge over the rockies looks better. Nevertheless, it seems that the envelope orography does not really improve the zonal mean component of the flow, the geopotentrial gradients around 40^0N still being too strong when compared to the Analysis.

3.2 Zonal mean steady flow and gravity wave drag

On Figure 6, the zonally averaged and time-averaged zonal wind from the same seasonal integrations and analyses as before are shown. At all levels, north of 40^oN, the zonal flow is too strong in the simulations with envelope orography (fig. 6b) when compared to the Analysis (Fig. 6a). By contrast the winds in the southern Hemisphere are more accurately simulated. This suggest that the model lacks a process of angular momentum transfert from the atmosphere to the earth, related to the orography. The fact that such a drag should be provided by gravity waves is strongly supported by the fact that the largest mean flow anomalies occur at high levels, near the polar tropopause (Palmer et al., 1986) . There, it is clear that the subtropical jet does not close in the forecasts when compared to the Analyses. The positive impact of such a gravity wave drag parameterization is illustrated on the Figure 6c where the zonal mean wind is shown for a series of long winter experiments with a gravity wave drag parameterization. This parameterization clearly gives an improved jet structure, with a weaker polar night jet. It also shows a large reduction in the westerlies in the lower stratosphere.

3.3 Impact on objective scores

As we have seen before, both the envelope orography and the gravity wave drag scheme have a beneficial impact on the model ability to simulate seasonal winter circulation. And the addition of these two processes have been found to give the

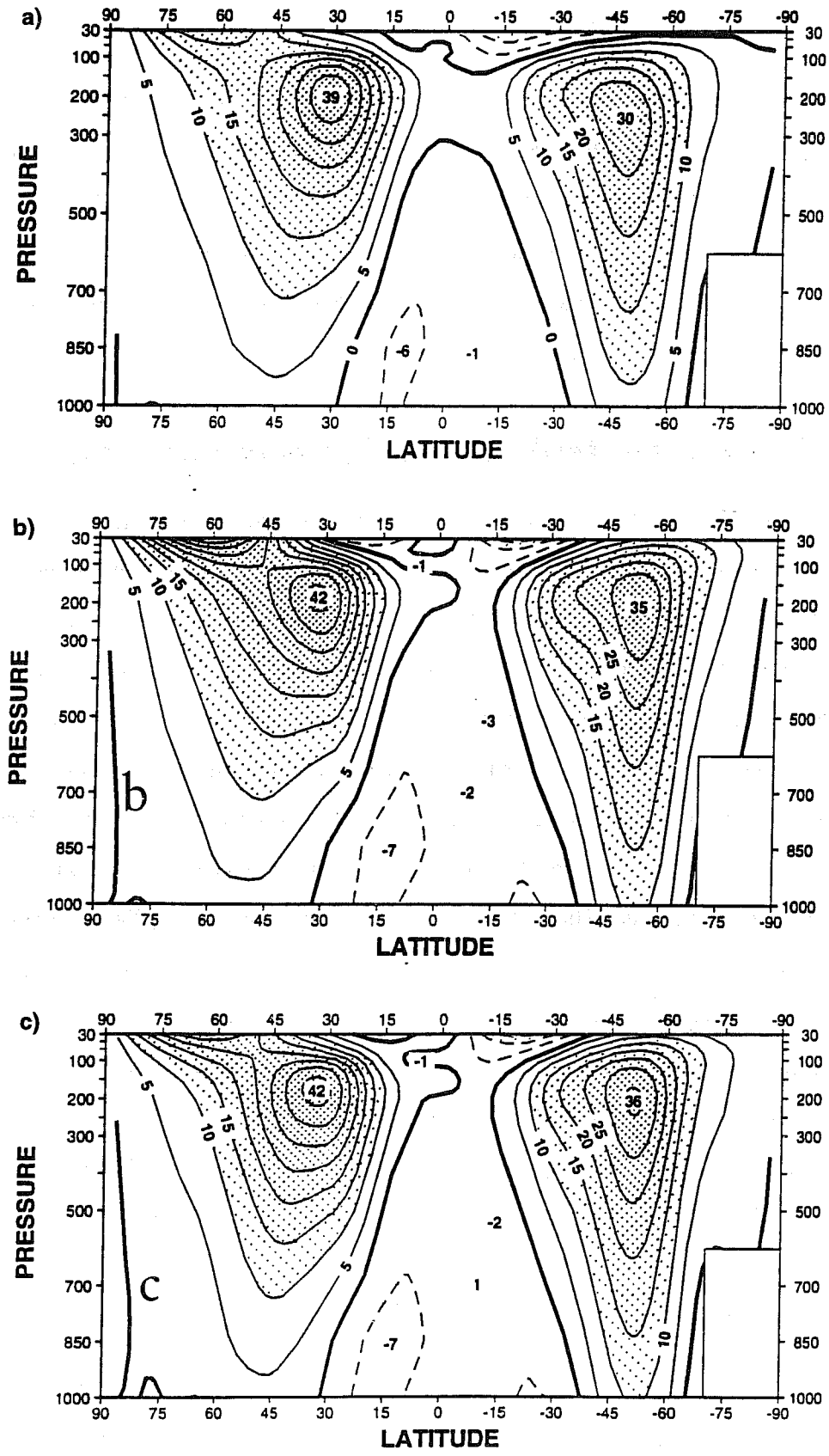

Fig 6 Northern Hemisphere climatic winter (Dec-Jan-Feb) zonal mean flow: winter mean averaged over 5 realisations. (a) Analysis (years 1986 to 1990). (b) Model runs with envelope orography 10 days of November 1990). (c) Model runs with envelope orography and gravity wave drag. In (b) and (c) the 5 forecasts correspond to 5 120 day realisations of the ECMWF T63L19 model starting 1, 2, 3, 4 and 5 November 1990. In these forecasts only the last 90 days are analysed to define the model climate.

best seasonal performances of the ECMWF model (Miller et al., 1989) . Nevertheless, since these parameterization mainly correct a slow drift of the model toward a too zonal too strong flow, it can not be expected that they have an significant impact on the very first days of a forecast. Nevertheless, at medium ranges, the slow drift aforementionned may become significant. The Figure 7 presents such diagnostics, where the ensemble objective scores of 3 sets containing 12 ten day forecasts at truncature T106L31, using the recent IFS forecast environment (CY11R7) are presented. The 12 experiments in each set correspond to twelve initial dates from 12 consecutive monthes (Avpril 1993 - Mars 1994). These include summer cases during which the gravity wave drag Scheme is known to have little impact on the forecast performances. Figure 7, shows that over the northern hemiphere, the envelope improves the Forecast skill in its medium range, in agreement with Wallace et al. (1983). Furthermore, the addition of the Gravity Wave Drag to the envelope still appears to be the best forecast configuration, in agreement with Miller et al. (1989).

3.4 Impact on the sub-synoptic scale dynamics

During the 1980's, the SSO parameterization have been introduced in order to reduce systematic errors in models, but they were strongly supported by theoretical studies and qualitatively justified by observational evidences. It is only recently (Bougeault et al., 1993) that real attempt to validate directly the SSO Schemes toward field data has been more systematically considered. For this reason it is not surprizing that Lott (1995) found a certain amount of irrealistics behaviour in the behaviour of the ECMWF mountain drag when compared to the drag measured during PYREX. Similarly, Bougeault et al. (1993) found that the present gravity wave drag in the ECMWF model has a too small amplitude and that it should be at least multiplied by a factor 4. Dynamical diagnostics of flow pattern observed during that campain further suggest that the mountain drag

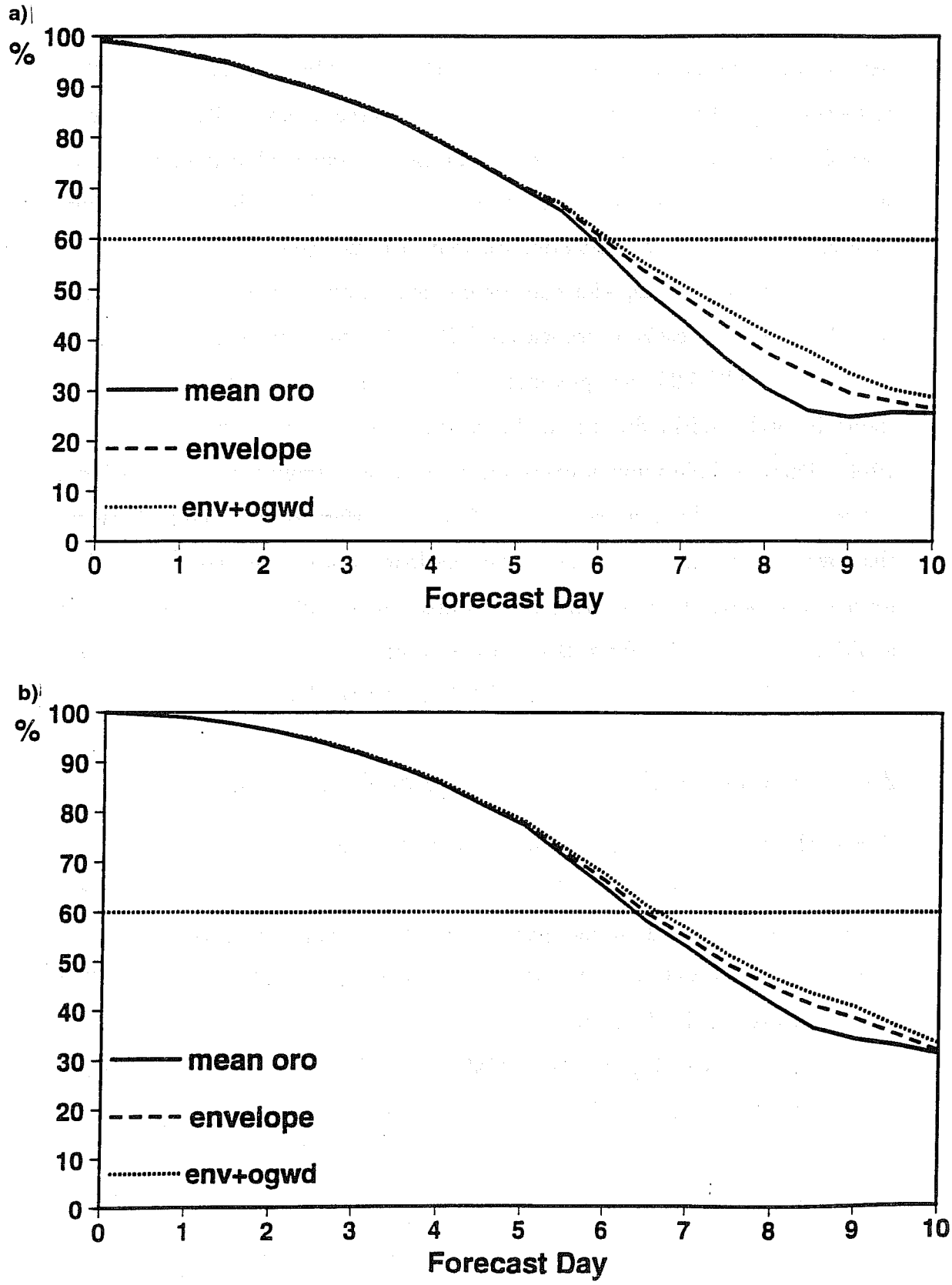

Fig 7 Mean anomaly correlation over twelve T106L31 forecasts starting every 15th of a year extending from March 1993 to April 1994. Northern Hemisphere, geopotential at 1000 mb (a), 500 mb (b). Continuous line: 12 forecasts with mean orography, dashed line: 12 forecasts with envelope orography, dotted line: 12 forecasts with envelope orography and gravity wave drag.

should mainly affect the flow located below and close to the actual mountain top, and that the envelope orography does not represent well this last effect (Lott, 1995) . This support our discussion in Section 2,where it was emphasized that nonlinear effects should be more systematically parameterized, slowing down the synoptic flow at levels located below and close to the actual mountain top. This study further show that low level drags have a beneficial impact on the model dynamics at the sub-synoptic range.

4 CONCLUSION

This study has illustrated that the orographic features which scales vary from 100m to 100km can play a significant role on the general circulation of the atmosphere. Among those scales, the longest (100Km-5Km) covers the gravity wave spectrum. In a GCM, for which the grid spacing is larger than 100Km, all those waves need to be parameterized. In NWPM which can have smaller gridspacing, part of this spectrum can be resolved explicitely by the model, but a significant amount remain to be parameterized. It was also shown that the USN dataset (with resolution of 10'x10') is not accurate enough to parameterize correctly the SSO gravity waves drag. Nevertheless, for realistic mountains, the linear hypothesis, upon which the gravity wave theory is based is rarely valid and nonlinear aspects of the dynamics which scale correspond to gravity waves have to be parameterized. In this nonlinear context, even smaller orographic features can slow down the large scale flow, through interaction between the boundary layer and the irregular bottom. These kind of small scall features are parameterized, to a certain extend, by increasing the roughness length over mountaneous areas. The concept of envelope orography, which stands that below the mountain peaks remain sheltered zones, where the atmosphere is at rest, can also be viewed as an artefact to simulate low level nonlinear effects.

In the present models the three different parametrization of the SSO (i.e.,

gravity wave drag, enhanced roughness length and envelope orography) have been developed rather independantly one from the other. As noticed in the introduction, this distinction is quite arbitrary. For instance, the increase of the roughness length above hilly regions results from study of neutral flow above orography. It is quite clear that in most of the cases of interest (i.e., winter over land), the stratification will modify significantly this theory. Typically, the theory will have to take into account gravity waves. On the other size, theoretical studies of mountain waves neglect the Boundary layer. This is really surprising since the nonlinear theory of mountain waves shows that those waves can break at rather low level and create turbulence. Similarly, theory of mountain waves (linear or non-linear) generally assumes a small slope, allthough this is generally not observed in reality. To summarize, The reality seems to be at a transition, in the nonlinear range (i.e., at large H_{ND}), between small slope configuration (theory of mountain waves with low level breaking or/and flow separation on the mountain flank) and large slope configuration (flow separation in the vertical direction and near the mountain peak) which is not really known. An other interaction between these different parameterizations which has not been discussed herein is that the envelope orography, by increasing the momentum transport by long waves, is also a form of gravity wave drag parameterization.

This discussion shows that there are plenty of theoretical reasons to parameterize the SSO in GCM and NWP. Nevertheless, these efforts in parameterizing the SSO in GCM are often fruitfull and in many cases, lead to improve the performances of the models. Typically, the envelope orography improves the structure of the planetary waves and the gravity wave drag the winter zonal mean jet in the polar tropopause. These two parameterization also give the best forecast performances. Nevertheless, there are still room too improve those different features. It is quite clear for instance that the steady planetary wave structure simulated in seasonal run is still too weak.

Acknowledgments

I would like to thank Dr L. Ferranti, Dr C. Brankovic and Dr M. Miller who made most of the seasonal integrations presented in the third section of this paper. I enjoyed very helpfull discussions on the interpretation of these integrations with these three colleagues as well as with Dr F. Molteni.

References

Bacmeister, J. T., and R. T. Pierrehumbert, 1988, On high drag states of nonlinear, stratified flow over an obstacle, *Journal of the Atmospheric Sciences*, *45*, 63–80, 1988.

Batchelor, G., *An introduction to fluid dynamics*, Cambridge University Press, 1967.

Boer, G., N. McFarlane, R. Laprise, J. Henderson, and J. Blanchet, 1984, The canadian climate centre spectral atmospheric general circulation model, *Atmos.-Ocean*, *22*, 397–429, 1984.

Bougeault, P., A. Jansa, J. Attie, I. Beau, B. Benech, B. Benoit, P. Bessemoulin, J. Caccia, J. Campins, and B. a. Carrissimo, 1993, The atmospheric momentum budget over a major mountain range: first results of the PYREX field program, *Annales Geophysicae*, *11*, 395–418, 1993.

Bretherton, F. P., 1969, Momentum transport by gravity waves, *Quarterly Journal of the Royal Meteorological Society*, *95*, 213–243, 1969.

Clark, T. L., and W. R. Peltier, 1984, Critical level reflection and the resonant growth of nonlinear moun tain waves, *Journal of the Atmospheric Sciences*, *41*, 3122–3134, 1984.

Durran, D. R., 1987, Another look at downslope winds. part 2: Nonlinear amplification beneath wave-overturning layers, *Journal of the Atmospheric Sciences*, *44*, 3402–3412, 1987.

Gill, A. E., *Atmosphere-ocean dynamics*, Academic Press, 1982.

Grant, A., and P. Mason, 1990, Observation of boundary layer structure over complex terrain, *Quarterly Journal of the Royal Meteorological Society*, *116*, 395–418, 1990.

Held, I. M., Stationary and quasi stationary eddies in the extratropical troposphere: theory, in *Large-scale dynamical processes in the atmosphere*, edited by B. Hoskins and R. Pearce, 127–168, Academic Press, 1983.

Lilly, D., J. Nicholls, R. Chervin, P. Kennedy, and J. Klemp, 1982, Aircraft measurements of wave momentum flux over colorado rocky moun tains, *Quarterly Journal of the Royal Meteorological Society, 108*, 625–642, 1982.

Lott, F., 1995, Comparison between the orographic response of the ECMWF model and the PYREX 1990 data, *Quarterly Journal of the Royal Meteorological Society, 0*, 1995.

Manabe, S., and T. Terpstra, 1974, The effect of mountains on the general circulation of the atmosphere as identified by numerical experiments, *JAS, 31*, 3–42, 1974.

Mason, P., On the parametrization of orographic drag, in *Seminar on Physical arameterization for numerical models of the atmosphere*, 139–165, ECMWF, 1985.

Miller, M., T. Palmer, and R. Swinbank, 1989, Parametrization and influence of subgridscale orography in general circulation and numerical weather prediction models, *Meteorology and Atmospheric Physics, 40*, 84–109, 1989.

Miranda, P. M. A., and I. James, 1992, Non-linear three dimensional effects on gravity-wave drag: splitting flow and breaking wave, *Quarterly Journal of the Royal Meteorological Society, 118*, 1057–1081, 1992.

Mobbs, S., 1994, unknown, *ECMWF Seminar Proceedings*, 1–10, 1994.

Palmer, T., G. Shutts, and R. Swinbank, 1986, Alleviation of systematic westerly bias in general circulation and numerical weather prediction models through an orographic gravity wave drag parametrization, *Quarterly Journal of the Royal Meteorological Society, 112*, 2056–2066, 1986.

Pierrehumbert, R. T., and W. B., 1985, Upstream effect of mesoscale mountains, *Journal of the Atmospheric Sciences, 42*, 977–1003, 1985.

Queney, P., *Theory of perturbations in stratified currents with application to airflow over mountains*, University of Chicago Press, 1947.

Smith, R., 1979, The influence of mountains on the atmosphere, *Advances in geophysics*, 87–230, 1979.

Swinbank, R., 1985, The global atmospheric angular momentum balance inferred from analyses made during the fgge, *Quarterly Journal of the Royal Meteorological Society, 111*, 977–992, 1985.

Taylor, P., 1977, Model predictions of neutrally stratified planetary boundary layer flow over ridges, *Boundary-Layer Meteorology, 107*, 111–120, 1977.

Tibaldi, S., and J. Geleyn, 1981, The production of a new orography, land-sea mask and associated climatological surface fields for operational purposes, *ECMWF Research Department, Technical Memorandum, 40*, 1981.

Volkert, H., 1990, An alpine orography resolving major valleys an massifs, *Meteorology and Atmospheric Physics, 43*, 231–234, 1990.

Wallace, J., S. Tibaldi, and A. Simmons, 1983, Reduction of systematic forecast errors in the ECMWF model through the introduction of an envelope orography, *Quarterly Journal of the Royal Meteorological Society, 109*, 683–717, 1983.

Wood, N., and P. Mason, 1993, The pressure force induced neutral, turbulent flow over hills, *Quarterly Journal of the Royal Meteorological Society, 119*, 1233–1267, 1993.